



## In-vitro Analysis of Antimicrobial Activities of Green Synthesized Silver Oxide Nanoparticles on some Microorganisms found in Open Wound

Rahama Orachachi Abdulmaleek<sup>1</sup>, Idongesit Edem Okon<sup>1,2\*</sup>, George Iloegbu Ndukwe<sup>1</sup>, Patricia Adamma<sup>1</sup>, E. Ekwumemgbo<sup>1</sup>

<sup>1</sup>Ahmadu Bello University, Zaria, Kaduna state, Nigeria

<sup>2</sup>Nigerian Institute of Transport Technology, Zaria, Nigeria

\*Correspondence: E-mail: [idokon22@yahoo.com](mailto:idokon22@yahoo.com)

### ABSTRACT

The main barrier to open wound healing is biofilm formation on the wound by a group of microbes encapsulated in a self-produced extracellular polymeric substance with high resistance to many conventional antimicrobial therapies. There is a need for unique anti-biofilm strategies and antimicrobial agents. This study aimed to investigate the antimicrobial activities of green synthesized silver oxide nanoparticles (Ag<sub>2</sub>O-NPs) on some bacteria (*Staphylococcus aureus*, *Bacillus subtilis*, *Escherichia coli*, and *Pseudomonas aeruginosa*) and fungi (*Candida albican*) commonly found in open wound (In-vitro). Ag<sub>2</sub>O-NPs exhibited considerable zone of inhibition (ZOI) against the test microorganisms. The minimum inhibitory concentration of silver nanoparticles against the bacteria was 3.75 and 15 mg/mL against the bacteria and fungi, respectively. The minimum bactericidal concentration was 7.50 and 15.00 mg/mL for bacteria and fungi, respectively. Green synthesized Ag<sub>2</sub>O-NPs exhibited some antimicrobial activities, which can aid in wound healing.

### ARTICLE INFO

#### Article History:

Submitted/Received 06 Jul 2024

First Revised 24 Aug 2024

Accepted 31 Oct 2024

First Available online 01 Nov 2024

Publication Date 01 Mar 2025

#### Keyword:

Antimicrobial activities,  
Green synthesized Ag<sub>2</sub>O-NPs,  
Inhibition zone,  
Minimum bactericidal  
concentration,  
Minimum inhibitory concentration,  
Wound.

## 1. INTRODUCTION

A wound can be defined as any discontinuity or break into the surface of epithelium due to any physical, chemical, or biological source (Kaushik et al., 2013). Wounds can be divided into two categories: acute wounds (such as surgical wounds and accidental wounds) and chronic wounds (such as venous leg ulcers, pressure ulcers, and diabetic foot ulcers (DFU) (Lindholm & Searle, 2016). The wound healing process incorporates several cellular and extracellular routes through overlapping phases, including the hemostasis/inflammatory phase, proliferative phase, and remodeling phase, to restore tissue integrity and functioning (Wang et al., 2018). The healing process is always opposed by micro-organisms, micro-organism or microbe is a microscopic organism, which may be multi-cellular or single-celled. Bacteria constitute a large domain of prokaryotic microorganisms, a large number exists on the skin and even more in the gut flora (Rappé & giovannoni, 2003). The vast majority of the bacteria in the body are rendered harmless by the protective effects of the immune system, though many are beneficial, particularly in the gut flora. However, several species of bacteria are pathogenic and cause infectious diseases such as cholera, syphilis, anthrax, leprosy, and bubonic plague. Some examples of bacteria found in wounds are *Staphylococcus aureus*, *Bacillus subtilis*, *Escherichia coli*, and *Pseudomonas aeruginosa* (Bessa et al., 2015; Ravindran et al., 2022).

*Staphylococcus aureus* (*S. aureus*) is a gram-positive cocci bacterium that is a member of the Firmicutes and is frequently found in the respiratory tract, genital tract, and on the skin. It is often positive for catalase and nitrate reduction and is a facultative aerobe that can grow without the need for oxygen (Heiland et al., 2016). *Bacillus subtilis* (*B. subtilis*) is a gram-positive bacterium, rod shaped and catalase positive. *B. subtilis* cells are about 4-10 micrometers (µm) long and 0.25-1.0 µm in diameter. *B. subtilis* is heavily flagellated, which gives it the ability to move quickly in liquids. *Escherichia coli* (*E. coli*) is a Gram-negative, facultative anaerobic, rod-shaped bacterium that is commonly found in the lower intestine of warm-blooded organisms. Most *E. coli* strains are harmless, but some serotypes can cause serious food poisoning in their hosts, and are occasionally responsible for product recalls due to food contamination. The harmless strains are part of the normal flora of the gut and can benefit their hosts by producing vitamin K 2 (Meganathan, 2001) and preventing colonization of the intestine with pathogenic bacteria.

*Pseudomonas aeruginosa* (*P. aeruginosa*) is a common Gram-negative, rod-shaped bacterium that can cause disease in plants and animals, including humans. *P. aeruginosa* is a prototypical “multidrug-resistant (MDR) pathogen” recognized for its ambiguity, its intrinsically advanced antibiotic resistance mechanisms, and its association with serious illnesses-especially nosocomial infections such as ventilator-associated pneumonia and various sepsis syndromes (Klockgether et al., 2011). *Candida albicans* is a dimorphic fungus that grows both as yeast and as filamentous cells. It is one of the few species of the *Candida* genus that cause the infection of candidiasis in humans (Erdogan & Rao, 2015). *C. albicans* is responsible for 50-90% of cases of candidiasis in humans, systemic fungal infections (fungemias) including those by *C. albicans* have emerged as important cases of morbidity and mortality in immune-compromised patients (e.g. AIDS, cancer chemotherapy, organ or bone marrow transplantation) (Martins-green et al., 2013).

Nanotechnology has gained massive applications in the fields of biology and pharmacology, nanotechnology is also used for the study of nanomaterials that exhibit amazing properties, functionalities, and phenomena due to the influence of small size (nanoscale) (Khan et al., 2019).

In wound treatment, there have been emergences of antimicrobial resistance pathogens and these have posed serious challenges. Silver nanoparticles (AgNP) have been an alternative to normal antibiotics, because of their effective antimicrobial actions against wound pathogens due to their notable properties like size, shape, and surface charge (Ravindran *et al.*, 2022).

Green-synthesized Ag<sub>2</sub>O-NPs have been more effective as an anti- antimicrobial agent against wound pathogens including (Ravindran *et al.*, 2022). This study therefore aimed at investigating the antimicrobial Activities of green synthesized and characterized silver oxide nanoparticles (Ag<sub>2</sub>O-NPs) from *Ocimum gratissimum* on some common wound microorganisms (*Staphylococcus aureus*, *Bacillus subtilis*, *Escherichia coli*, and *Pseudomonas aeroginosa*, and *Candida albican*).

## 2. METHODS

### 2.1. Materials

The Green Synthesized Silver Oxide Nanoparticles (Ag<sub>2</sub>O-NPs) used were from the synthesis carried out by Abdulmaleek *et al.* (2023). The test organisms used for this analysis were micro-organisms (bacteria and fungi) commonly found in wounds (Bessa *et al.*, 2015) that were clinically isolated, identified, and characterized at the Department of Microbiology, Faculty of Life Sciences, Ahmadu Bello University, Zaria. The isolates were: two (2) Gram-positive bacterial strains- *Staphylococcus aureus* and *Bacillus subtilis*; two (2) Gram-negative bacterial strains- *Escherichia coli* and *Pseudomonas aeroginosa*; one (1) fungal strain- *Candida albican*. The antimicrobial test was carried out in the Department of Microbiology, Ahmadu Bello University, Zaria by the Laboratory standard as reported by Offiong and Martelli (1994).

### 2.2. Characterization of the green synthesized Ag<sub>2</sub>O-NPs

Characterization of the green synthesized Ag<sub>2</sub>O-NPs was carried out using UV–Vis spectroscopy, Scanning Electron Microscopy (SEM), X-ray diffraction (XRD), Energy Dispersive X-ray Spectroscopy (EDX), and Fourier Transform Infrared Spectroscopy (FTIR) as was done by Abdulmaleek *et al.* (2023).

### 2.3. Culture media

The culture media used for the analysis include Mueller Hinton Agar (MHA), Mueller Hinton-Broth (MHB), Potato Dextrose Agar (PDA), and Nutrient Agar (NA). These media were used for sensitivity tests, minimum inhibitory concentration, and minimum bactericidal concentration (MBC). All media were prepared according to the manufacturer's instructions as recommended by the 2011 Clinical and Laboratory Standards Institute guidelines (Pereira *et al.*, 2009) and they were sterilized by autoclaving at 120°C for 15 min.

### 2.4. Inoculums preparation

The bacterial isolates were first grown in a nutrient broth for 18 hours before use. The microbial inoculums were standardized by 0.50 McFarland turbidity standard scale number (comparable to a bacterial suspension of 10<sup>8</sup> cells per/cm<sup>3</sup>. The standard was compared visually to a suspension of bacteria in nutrient broth accordingly) to give a turbid solution; this was done by using a sterile inoculating loop touch; isolated colonies of the same morphology was suspended in 5.00 cm<sup>3</sup> of nutrient broth in a sterile test tube for the identified bacteria. McFarland turbidity standards of scale number 0.50 were vigorously agitated to turbidity on a vortex mixer before use.

## 2.5. Determination of inhibitory activity (Sensitivity Test) of the silver nanoparticles using the Agar Well- Diffusion Method

The antimicrobial screening was carried out using the agar well-diffusion method as described by Humphries *et al.*, (2021). The standardized inocula of both the bacterial and fungal isolate were streaked on sterilized Mueller Hinton and Potato dextrose agar plates respectively with the aid of sterile swab sticks, four wells were punched on each inoculated agar plate with a sterile cork borer. The well was properly labeled according to different concentrations of the Ag<sub>2</sub>O-NPs prepared, which were by serial diffusion of 60, 30, 15, and 7.5 mg/cm<sup>3</sup> respectively. Each well was filled up with 0.20 cm<sup>3</sup> of the Ag<sub>2</sub>O-NPs. The inoculated plates were allowed to stay on the bench for 1 hour; this was to enable the Ag<sub>2</sub>O-NPs to diffuse into the agar. The plates were then incubated at 37°C for 24 hours (plates of Mueller Hinton agar) while the plates of potato dextrose agar were incubated at room temperature for about 72 hours.

At the end of the incubation period, the plates were observed for any evidence of inhibition completely devoid of growth around the wells (zone of inhibition). The diameters of the zones were measured using a transparent ruler calibrated in centimeters and the results were recorded.

## 2.6. Determination of minimum inhibitory concentration (MIC)

The minimum inhibitory concentration of the Ag<sub>2</sub>O-NPs was determined using the tube dilution method with the Mueller Hinton broth used as diluents. The lowest concentration of the Ag<sub>2</sub>O-NPs (7.50 mg/cm<sup>3</sup>) showing inhibition for each organism during the sensitivity test was serially diluted in the test tubes containing Mueller Hinton broth. The standardized organisms were inoculated into each tube containing the broth and Ag<sub>2</sub>O-NPs. The inoculated tubes were then incubated at 37°C for 24 hours. At the end of the incubation period, the tubes were examined or observed for the presence or absence of growth using turbidity as a criterion. The lowest concentration in the series without visible signs of growth (turbidity) was considered to be the minimum inhibitory concentration (MIC).

## 2.7. Determination of minimum bactericidal concentration (MBC)

The result from the minimum inhibitory concentration (MIC) was used to determine the minimum bactericidal concentration (MBC) of the extract. A sterilized wire loop was dipped into the test tubes that did not show turbidity (clear) in the MIC test and a loopful was taken and streaked on sterile nutrient agar plates. The plates were incubated at 37°C for 24 hours.

At the end of the incubation period, the plates were examined or observed for the presence or absence of growth. This was to determine whether the antimicrobial effect of the Ag<sub>2</sub>O-NPs is bacteriostatic or bactericidal.

## 3. RESULTS AND DISCUSSION

### 3.1. Characterization of the green synthesized silver oxide nanoparticles (Ag<sub>2</sub>O-NPs)

The synthesized Ag<sub>2</sub>O-NPs were characterized by the application of UV–Vis spectroscopy, Scanning Electron Microscopy (SEM), X-ray diffraction (XRD), Energy Dispersive X-ray Spectroscopy (EDX), and Fourier Transform Infrared Spectroscopy (FTIR), Characterization was carried out by Abdulmaleek *et al.* (2023). UV–visible spectroscopy was carried out using an Agilent Cary 300 U.V spectrophotometer within the spectra range of 200–800 nm (**Figure 1**). The absorbance peak was observed at 261 nm due to surface plasmon resonance corresponding to nanoparticles' presence, revealing the reduction of AgNO<sub>3</sub> to Ag<sub>2</sub>O-NPs. The

261 nm peak is low compared to 430-433 nm observed by [Ajayi et al. \(2014\)](#). This could emanate from the Ag<sub>2</sub>O-NPs average size obtained in this study as evidenced in the report by [Shume et al. \(2020\)](#), where maximum absorption connects with particle size. Scanning Electron Microscope coupled on EDX detector; Model Supra TM 35 VP (Carl Zeiss instrument, United Kingdom) was used to determine the surface morphology and size of the Ag<sub>2</sub>O-NPs synthesized (**Figure 2**). The Ag<sub>2</sub>O-NPs were spherical and well distributed with a size range of 20 – 100 nm, the spherical shape aligns with [Sultan et al. \(2023\)](#).

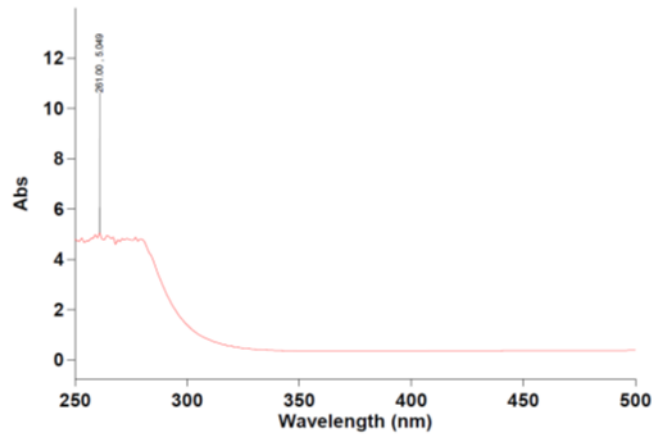


**Figure 1.** UV-Visible Spectroscopy of the Green Synthesised Ag<sub>2</sub>O-NPs ([Abdulmaleek et al., 2023](#)).

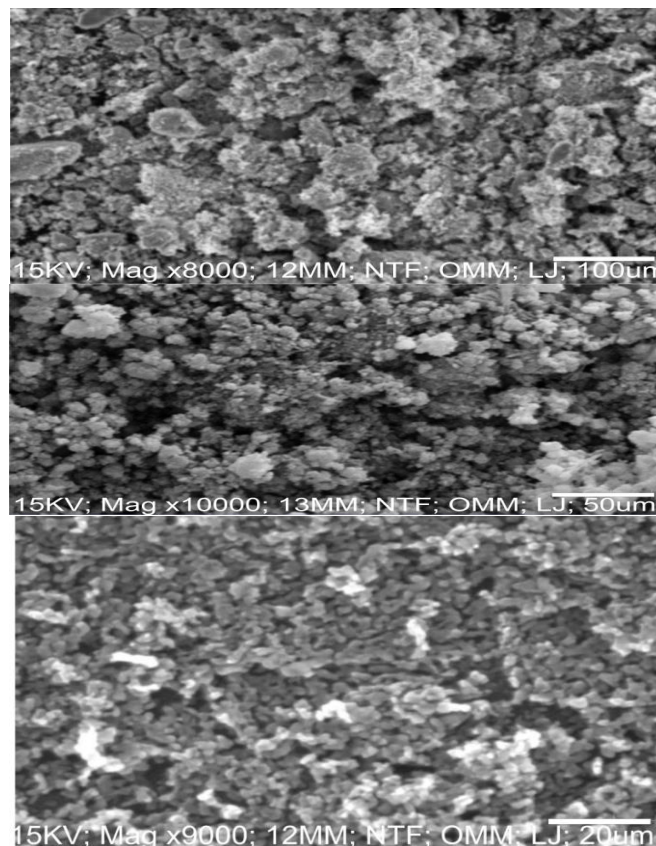


**Figure 2.** SEM Micrograph of the Green Synthesised Ag<sub>2</sub>O-NPs at various Magnifications ([Abdulmaleek et al., 2023](#)).

The structure of the green synthesized  $\text{Ag}_2\text{O}$ -NPs was determined through X-ray diffraction (XRD) analyses using an X-ray diffractometer with  $\text{Cu } \alpha$  radiation ( $\lambda = 0.15406 \text{ nm}$ ) over the scanning range of  $2\theta = 5\text{--}80^\circ$  (**Figure 3**). The XRD pattern shows several peaks, the two main peaks located at  $33.93$  and  $38.61^\circ$  correspond to (100) and (101) planes of the face-centered cubic (FCC) crystalline structure in line with those recorded in the Joint Committee on Powder Diffraction Standards (JCPDS, card No. 04-0783) for the characteristic face-centered cubic structure of  $\text{Ag}_2\text{O}$ -NPs. This centered cubic structure for green synthesized  $\text{Ag}_2\text{O}$ -NPs was also observed by [Fayyadh and Alzubaidy et al. \(2021\)](#). The elemental composition of the green synthesized  $\text{Ag}_2\text{O}$ -NPs was determined using energy-dispersive X-ray (EDX) Spectroscopy. Silver (Ag), Oxygen (O), and carbon (C) were the elements observed, with compositions of 80, 10.26, and 9.74% respectively (**Figure 4**). The composition discloses the high purity of the green synthesized  $\text{Ag}_2\text{O}$ -NPs. Spectra obtained from Fourier transforms infrared (FTIR) spectroscopy are presented in **Figure 5**. Typical bands at  $3686\text{--}3626 \text{ cm}^{-1}$  correspond to the O-H stretching of alcohol,  $3140$  corresponds to the O-H stretching of carboxylic acid, and  $2000.67 \text{ cm}^{-1}$  corresponds to the C-H bending of aromatic compounds.  $1614.56 \text{ cm}^{-1}$  corresponds to the N-H bending of amine, and  $1310.30$  indicates the C-N stretching of aromatic amine.  $797.73 \text{ cm}^{-1}$  corresponds to the C-Cl stretching of alkyl halides. The numerous peaks at  $475.51\text{--}415.14 \text{ cm}^{-1}$  correspond to Ag-O stretching, and this confirms the presence of  $\text{Ag}_2\text{O}$ -NPs ([Abdulmaleek et al., 2023](#)).

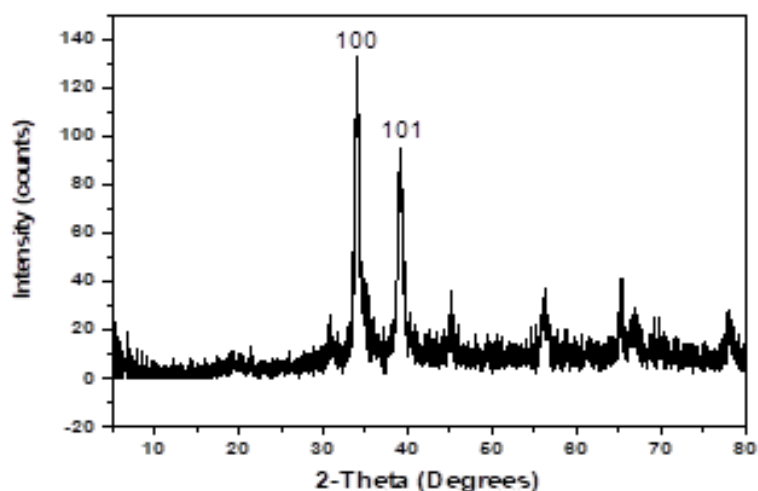


**Figure 3.** XRD pattern of the Green Synthesized  $\text{Ag}_2\text{O}$ -NPs ([Abdulmaleek et al., 2023](#)).

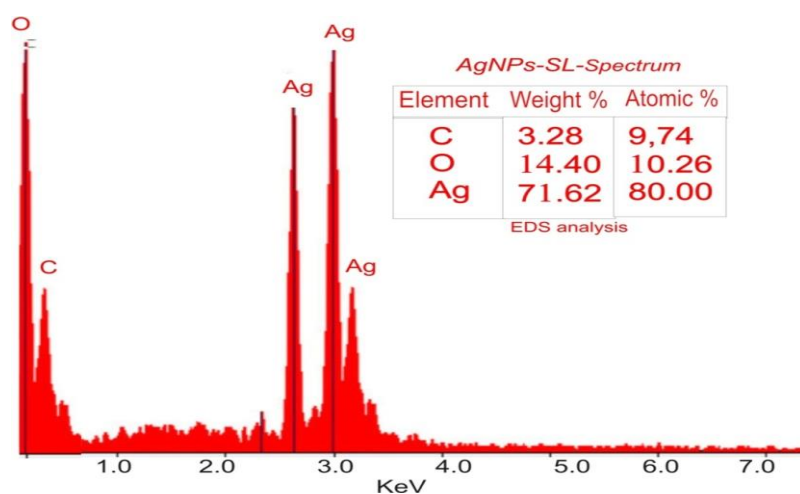


**Figure 4.** EDX Spectra of the Green Synthesized  $\text{Ag}_2\text{O}$ -NPs ([Abdulmaleek et al., 2023](#)).

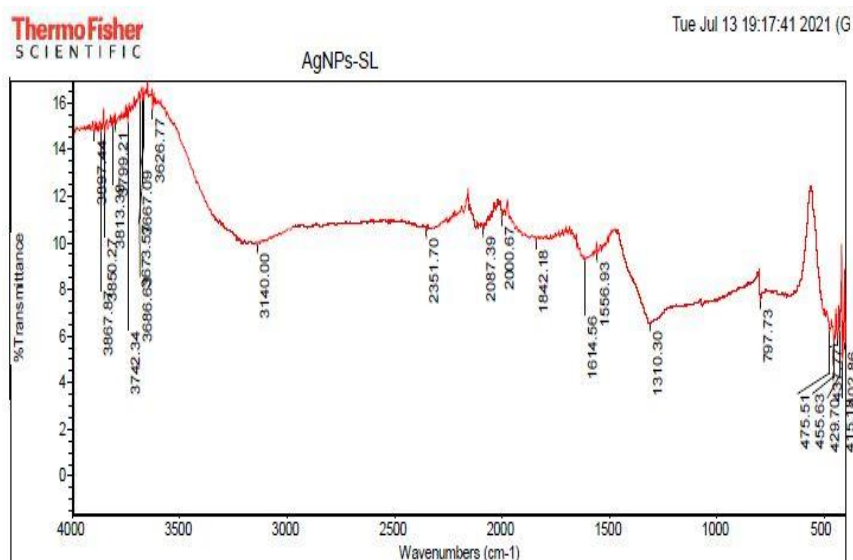


Figure 5. FTIR Spectra of the Green Synthesized Ag<sub>2</sub>O-NPs (Abdulmaleek *et al.*, 2023).

### 3.2. Antimicrobial activity of the green synthesized Ag<sub>2</sub>O-NPs

The antimicrobial activity of the green synthesized Ag<sub>2</sub>O-NPs was analyzed by determination of inhibition zone, minimum inhibitory concentration (MIC), and minimum bactericidal concentration (MBC). Figures 6, 7, 8, 9, and 10, respectively, present antimicrobial test of the Ag<sub>2</sub>O-NPs on the different microbes- *Staphylococcus aureus*, *Bacillus subtilis*, *Escherichia coli*, *Pseudomonas aeruginosa* and *Candida albican*.

The inhibition zone denotes the area on an agar plate where the growth of a control organism is prevented by an antibiotic usually placed on the agar surface. If the test microorganism is susceptible to the antibiotic agent used, it will not grow where the antibiotic is present or very close to it. The size of the zone of inhibition is a measure of the antibiotic agent effectiveness, the larger the clear area around the antibiotic agent, the more effective it is. MIC is the lowest concentration in mg/L or µg/µL of an antimicrobial agent that inhibits the visible growth of microorganisms in-vitro after 24 hours of incubation, while **MBC otherwise** termed minimum lethal concentration (MLC) is the lowest concentration of antibiotics that can kill or prevent the growth of the inoculum up to 99.9%.



Figure 6. Antimicrobial Activity of the Ag<sub>2</sub>O-NPs on *Staphylococcus aureus*

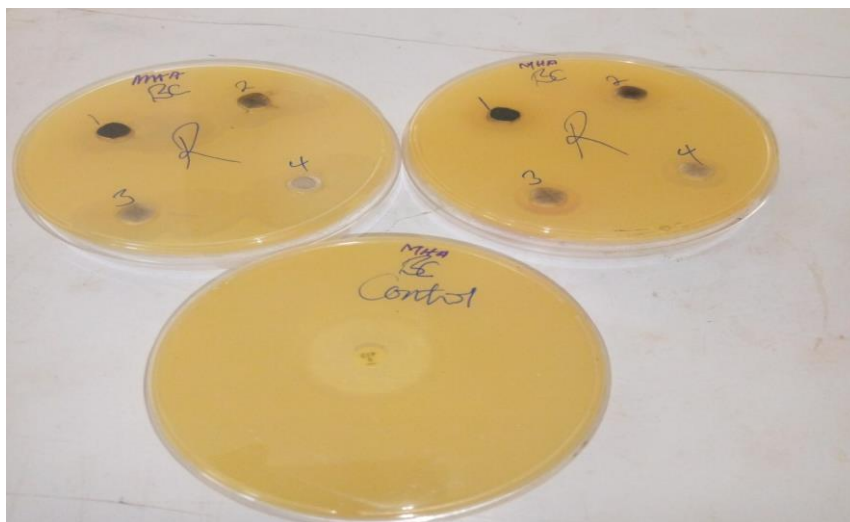


**Figure 7.** Antimicrobial Activity of the Ag<sub>2</sub>O-NPs on *Bacillus subtilis*



**Figure 8.** Antimicrobial Activity of the Ag<sub>2</sub>O-NPs on *Escherichia coli*

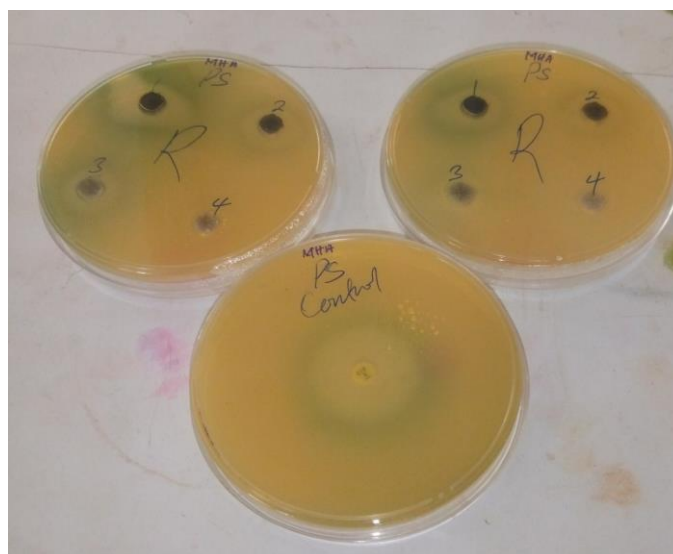


**Figure 9.** Antimicrobial Activity of Ag<sub>2</sub>O-NPs on *Pseudomonas aeruginosa*.

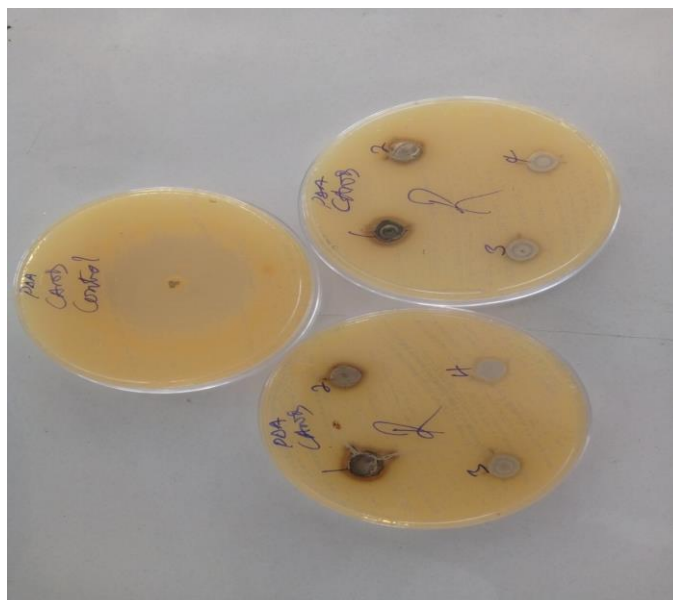


**Figure 10.** Antimicrobial Activity of the Ag<sub>2</sub>O-Nps on *Candida albican*

### 3.2.1. Zone of inhibition (ZOI)

Microbial activity of the green synthesized Ag<sub>2</sub>O-NPs concerning zone inhibitions were observed after 24 hours for each of the microbes as illustrated in **Figures 6-10** respectively and presented in **Table 1**. The maximum concentration of the Ag<sub>2</sub>O-NPs (60 mg/cm<sup>3</sup>) gave the largest zone of inhibition (ZOI) for all the microbes and was observed to be 21.10, 14.70, 19.05, 17.85, and 14.20 mm for *S. aureus*, *B. subtilis*, *E.coli*, *P. aeruginosa* and *C. albican* respectively (**Table 1**). At the same concentration of 60 mg/cm<sup>3</sup>, ZOI of 35.00, 25.05, 24.50, 27.00, and 39.90 mm were observed for the Control (Ciprofloxacin) respectively. Furthermore, the green synthesized Ag<sub>2</sub>O-NPs did not demonstrate a zone of inhibition greater than that of the Control on any of the microorganisms and at all concentrations. Despite this, the ZOI exhibited by the green synthesized Ag<sub>2</sub>O-NPs against the microbes has proven that it has substantial antimicrobial properties.

The largest zones of inhibition of 21.10 mm, 20.15 mm, 18.70 mm, and 17.15 mm at different concentrations (mg/cm<sup>3</sup>) of 60, 30, 15, and 7.5 respectively were observed for *S. aureus* (a Gram-positive bacterium). However, *E.coli* and *P. aeruginosa* (Gram-negative bacteria) exhibited higher zones of inhibition across all concentrations compared to *B. subtilis* (Gram-positive bacterium). This suggests that Gram-negative bacteria could be more susceptible to Ag<sub>2</sub>O-NPs compared to Gram-positive bacteria. The higher susceptibility of Gram-negative bacteria to silver nanoparticles as compared to Gram-positive bacteria has been reported ([Ahluwalia et al., 2018](#); [Ramesh et al., 2015](#)). This difference could be explained by variations in the composition of the cell walls of Gram-positive and Gram-negative bacteria. In Gram-positive bacteria, the cell wall is constituted of a thick peptidoglycan layer, consisting of short peptide cross-linked linear polysaccharide chains, leading to a more rigid structure, increasing difficulties in penetration of the Ag<sub>2</sub>O-NPs. On the other hand, the Gram-negative bacteria's cell wall is composed of a thinner peptidoglycan layer.

### 3.2.2. Minimum inhibitory concentration (MIC)

After analyzing the zone inhibition activity of the green synthesized Ag<sub>2</sub>O-NPs on the microbes (*Staphylococcus aureus*, *Bacillus subtilis*, *Pseudomonas aeruginosa*, *Escherichia coli*, and *Candida albican*), MIC of the Ag<sub>2</sub>O-NPs was determined against each of the microbes. The

results proved that the MIC value of silver nanoparticles against the selected bacteria varied and this variability depends upon the bacterial strains. The minimum inhibitory concentration value of silver nanoparticles against the bacteria was 3.75 mg/cm<sup>3</sup> for *Staphylococcus aureus*, *Bacillus subtilis*, *Escherichia coli*, and *Pseudomonas aeruginosa*. The MIC value for the fungus (*Candida albican*) was 15 mg/cm<sup>3</sup>. MIC results relate to the fact that a larger zone of inhibition corresponds to a smaller minimum inhibitory concentration as was reported by [Mohanty et al. \(2010\)](#).

### 3.2.3. Minimum bactericidal concentration (MBC)

The minimum bactericidal concentration results confirmed that the green synthesized Ag<sub>2</sub>O-NPs have bacterial growth inhibition properties. The MBC result for all the bacterial strains is 7.5 mg/cm<sup>3</sup> (*Staphylococcus aureus*, *Bacillus subtilis*, *Escherichia coli*, *Pseudomonas aeruginosa*) while it was 30 mg/cm<sup>3</sup> for the fungi (*Candida albican*) as shown in **Table 1**.

**Table 1.** Antimicrobial activities of the Ag<sub>2</sub>O-NPs on microbes

Test Samples	Zone of Inhibition (mm)				Control (Cipro ofloxacin)	MIC (mg/cm <sup>3</sup> )	MBC (mg/cm <sup>3</sup> )
	Different concentrations of Ag <sub>2</sub> O-NPs (mg/cm <sup>3</sup> )						
	60	30	15	7.5			
<i>S. aureus</i>	21.10	20.15	18.70	17.15	35.00	3.75	7.50
<i>B. subtilis</i>	14.70	14.25	13.05	12.25	25.05	3.75	7.50
<i>E.coli</i>	19.05	15.75	14.70	13.00	24.50	3.75	7.50
<i>P. aeruginosa</i>	17.85	16.65	16.00	15.05	27.00	3.75	7.50
<i>C. albican</i>	14.20	12.90	10.85	9.10	39.90	15.00	30.00

MIC= Minimum Inhibitory Concentration; MBC= Minimum Bactericidal Concentration

## 4. CONCLUSION

The green synthesized silver nanoparticles (Ag<sub>2</sub>O-NPs) were found to possess some antimicrobial properties. The zone inhibition exhibited by the green synthesized Ag<sub>2</sub>O-NPs against test organisms linked to the wound revealed that it could aid in wound healing. However, clinical trials are needed for further justification. Green synthesis if well harnessed, the use of hazardous chemicals could be avoided for both health and environmental safety.

## 5. AUTHORS' NOTE

The authors declare that there is no conflict of interest regarding the publication of this article. Authors confirmed that the paper was free of plagiarism.

## 6. REFERENCES

- Abdulmaleek, R.O., Ndukwe, G.I., Okon, I.E., and Ekwumemgbo, P.A. (2023). Green route synthesis and characterization of silver oxide nanoparticles using ocimum gratissimum leaf extract. *Journal of Materials and Environmental Science*, 14(12), 1494-1503.
- Ahluwalia, V., Sasikumar, E., Kumar, V., Kumar, S., and Sangwan, R.S. (2018). Nano silver particle synthesis using swertia paniculata herbal extract and its antimicrobial activity. *Microbial Pathology*, 114, 402-408.

- Ajayi, A.M., Tanayen, J.K., Ezeonwumelu, J.O.C., Dare, S., Okwanachi, A., Adzu, B., and Ademowo, O.G. (2014). Anti-inflammatory, anti-nociceptive and total polyphenolic content of hydroethanolic extract of ocimum gratissimum L. leaves. *African Journal of Medicine and Medical Sciences*, 43(1), 215-225.
- Bessa, L.J., Fazii, P., Di Giulio, M., and Cellini, L. (2015). Bacterial isolates from infected wounds and their antibiotic susceptibility pattern: Some remarks about wound infection. *International Wound Journal*, 12(1), 47-52.
- Erdogan, A., and Rao, S.S.C. (2015) Small intestinal fungal overgrowth. *Current Gastroenterology Reports*, 17(4), 1-7.
- Fayyadh, A.A., and Alzubaidy, M.H.J. (2021) Green-synthesis of Ag2O nanoparticles for antimicrobial assays. *Journal of the Mechanical Behavior of Materials*, 30, 228–236.
- Heiland, D.H., Masalha, W., Franco, P., Machein, M.R., and Weyerbrock, A. (2016). Progression-free and overall survival in patients with recurrent glioblastoma multiforme treated with last-line bevacizumab versus bevacizumab/lomustine. *Journal of Neuro-oncology*, 126, 567-575.
- Humphries, R., Bobenchik, A.M., Hindler, J. A., and Schuetz, A.N. (2021). Overview of changes to the clinical and laboratory standards institute performance standards for antimicrobial susceptibility testing, M100. *Journal of Clinical Microbiology*, 59(12), e00213-21.
- Kaushik, D., Kamboj, S., Kaushik, P., Sharma, S., and Rana, A. (2013). Burn wound: Pathophysiology and its management by herbal plants. *Chronicles of Young Scientists*, 4(2), 86-86.
- Khan, I., Saeed, K., and Khan, I. (2019). Nanoparticles: Properties, applications and toxicities. *Arabian Journal of Chemistry*, 12(7), 908-931.
- Klockgether, J., Cramer, N., Wiehlmann, L., Davenport, C.F., and Tümmler, B. (2011). *Pseudomonas aeruginosa* genomic structure and diversity. *Frontiers in Microbiology*, 2, 150.
- Lindholm, C., and Searle, R. (2016). Wound management for the 21st century: Combining effectiveness and efficiency. *Intenational Wound Journal*, 13, 5-15.
- Martins-Green, M., Petreaca, M., and Wang, L. (2013). Chemokines and their receptors are key players in the orchestra that regulates wound healing. *Advances in Wound Care*, 2(7), 327-347.
- Meganathan, R. (2001). Biosynthesis of menaquinone (vitamin K2) and ubiquinone (coenzyme Q): A perspective on enzymatic mechanisms. *Vitamins and Hormones*, 61, 173-218.
- Mohanty, A., Das, C., Dash, S., and Sahoo, D.C. (2010). Physico-chemical and antimicrobial study of poly herbal formulation. *International Journal of Comprehensive Pharmacy*, 4(4), 1-4.
- Offiong, O.E., and Martelli, S. (1994). Antibacterial activity of metal complexes of benzyl and benzoin thiosemicarbazones. *Societa Chimica Italiana*, 49(7-8), 513-518.
- Pereira, V., Lopes, C., Castro, A., Silva, J., Gibbs, P., and Teixeira, P. (2009). Characterization for enterotoxin production, virulence factors, and antibiotic susceptibility of

staphylococcus aureus isolates from various foods in Portugal. *Food Microbiology*, 26(3), 278-282.

Ramesh, P.S., Kokila, T., and Geetha, D. (2015). Plant mediated green synthesis and antibacterial activity of silver nanoparticles using emblica officinalis fruit extract. *Spectrochimica Acta Part A: Molecular and Biomolecular Spectroscopy*, 142, 339-343.

Rappé, M.S., and Giovannoni, S.J. (2003). The uncultured microbial majority. *Annual Reviews in Microbiology*, 57(1), 369-394.

Ravindran, E.R.S., Shanmugam, K., Veeramani, S., Ilangovan, R., Ali, D., Almutairi, B.O., Palanivel, H., and Goel, M. (2022). Effect of phytofabricated silver oxide nanoparticles on wound pathogens. *Journal of Nanomaterials*, 2022(1), 1760829.

Shume, W.M., Murthy, H.A., and Zereffa, E.A. (2020). A review on synthesis and characterization of Ag<sub>2</sub>O nanoparticles for photocatalytic applications. *Journal of Chemistry*, 2020(1), 5039479.

Sultan, A.E., Abdullah, H.I., and Niama, A.H. (2023). Synthesis of silver oxide nanoparticles using different precursor and study cytotoxicity against MCF-7 breast cancer cell line. *Nanomedicine Research Journal*, 8(3), 259-267.

Wang, P.H., Huang, B.S., Horng, H.C., Yeh, C.C., and Chen, Y.J. (2018). Wound healing. *Journal of the Chinese Medical Association*, 81, 94–101.